Contents list available at IJRED website

International Journal of Renewable Energy Development

Journal homepage: https://ijred.undip.ac.id

Research Article

The Conductivity Enhancement of $1.5Li_2O$-P_2O_5 Solid Electrolytes by Montmorillonite Addition

Yustinus Purwamargapratala[a,b*], Anne Zulfia Syahrial[a], Teguh Yulius Surya Panca Putra[b], Evvy Kartini[b], Heri Jodi[b]

[a]*Department of Metallurgy and Materials Engineering, University of Indonesia, UI Depok Campus, West Java 16424, Indonesia*

[b]*National Research and Innovation Agency (BRIN), Puspiptek National Science Technopark, South Tangerang, Banten 15314, Indonesia*

Abstract. Most solid electrolyte materials have not shown enough conductivity to be used as an electrolyte for a battery in electronic devices. The mixture of 1.5 Li_2O and P_2O_5 has been reported to show a good conductivity higher than that of Li3PO4, which is thought to be due to phase mixtures that are formed during manufacturing process. Montmorillonite (MMT) was used to explore the effect of phase mixture on conductivity of new 1.5Li2O-P2O5-MMT solid electrolyte composite, which was prepared through conventional solid-state reaction procedures. This study was conducted, how the addition of MMT affects process of forming $1.5Li_2O$-P_2O_5-MMT compound, and whether it influences electrical properties and permittivity of compound. Morphology, hygroscopicity, and electrochemical characteristics of this material were analyzed in this study. The shape of glassy-like flakes was reduced in micrographs, and granular lumps were getting larger as MMT was added. Addition also tended to reduce hygroscopicity, as indicated by a reduced rate of porous absorption. Whole Nyquist plot consisted of only one imperfect semicircular arc, indicating only one relaxation process occurred in materials. Capacitance of all arcs indicated main contribution of response was from bulk material. Slope of dielectric loss of samples indicated that conduction in the samples was mainly dominated by dc conduction. MMT clays acted as a medium that absorbed liquid phase in solid-state reaction, increasing formation of dominant phase, which determined total conductivity of compound. Conductivity was higher than that of $Li_4P_2O_7$, where the sample of 20 wt% MMT addition was most polarizable and most dielectric compound.

Keywords: Lithium Phosphate, Li_2O-P_2O_5, solid electrolyte, Montmorillonite, conductivity, Electrochemical Impedance Spectroscopy

Received: 5th July 2022; Revised: 15th Nov 2022; Accepted: 4th Dec 2022; Available online: 18th Dec 2022

1. Introduction

Batteries play a very important role, both as energy storage devices, and as energy suppliers, in electrical and electronic devices. However, research on batteries has not yet found Lithium-ion battery specifications that meet the application requirements, namely high energy density, long service life, good safety factors, and wide usage temperature range (Koniak & Czerepicki, 2017). Researchers broadly see the aspects in the battery that make it possible to improve its performance, including electrolyte material, stable electrode material, high energy density, additives, binders, current collector, and efficient packaging (Oleg *et al,* 2022). Among these aspects, electrolytes play an important role in the development of battery technology.

Traditional batteries, such as lithium-ion batteries in mobile phones, generally depend on the flow of charge in a liquid electrolyte made of lithium salt solution in organic solvents. This will cause an irreversible decrease in the capacity, as a result of the formation of a stable layer between the electrodes and electrolytes, which is often called the Solid Electrolyte Interphase (SEI). In addition, the use of liquid electrolytes also inhibits the increase in the battery life cycle, limits the temperature range of use, makes packaging difficult, and causes leakage, and safety problems in the batterie (Lin *et al.*, 2020). Therefore, the utilization of solid inorganic electrolytes with high thermal stability is an interesting choice to replace liquid organic electrolytes, to solve problems related to loss of capacity, lifetime, and safety issues (Sahu *et al.,* 2014; Purwamargapratala *et al.,* 2020). Because it has the same function as liquid electrolytes, some conditions absolutely must be met by solid electrolyte materials, including having high room temperature conductivity, negligible electronic conductivity with high ionic transfer value, and considerable electrochemical stability (Kaur *et al.*, 2021). One important requirement for obtaining high ionic conduction is that the microstructure of solid ionic material has disorders, which can be attempted by raising the temperature to increase the number of intrinsic defects, or by adding impurities to create vacancies or defects in the structure (Hou *et al.*, 2018). In general, solid electrolytes have advantages in terms of ease of design to make greater battery density, do not cause leakage, and have better resistance to collisions and vibrations (Guo *et al.*, 2022). Solid electrolytes are also conductors which only deliver one type of charge so during operation are very beneficial to reduce the overpotential of the cells (Quartarone and Mustarelli, 2011; Ohno *et al.*, 2021). In addition, solid electrolytes show better electrochemical stability and good compatibility with higher potential cathodes for increasing their energy density (Xiayin *et al.*, 2016). Moreover, some solid electrolytes have a

* Corresponding author:
Email: yust002@brin.go.id (Y. Purwamargapratala)

https://doi.org/10.14710/ijred.2023.47425
ISSN: 2252-4940/© 2023.The Author(s). Published by CBIORE

conductivity value equivalent to liquid electrolytes, with negligible electronic conductivity values (Kartini *et al.*, 2014).

Phosphate oxide-based electrolytes attract a lot of attention to be applied as solid electrolytes, ceramic glass, amorphous semiconductors, and optoelectronic devices (Kartini *et al.*, 2014). This conductor material is relatively easy to prepare, resistant to heat and vibration, has a large coefficient of heat expansion, and the choice of composition is varied (Das *et al.*, 2008). However, its use has become very limited due to its poor chemical resistance. Therefore, the development of phosphate-based conductors that are modified into alloys or composites, is an interesting thing to do further.

The Li_2O-P_2O_5 system has three polymorphs that can be prepared through the reaction of melt-quench solids, as shown in the Nakano phase diagram (Masaki *et al.*, 2022), namely Lithium Orthophosphate Li_3PO_4, Lithium Pyrophosphate $Li_4P_2O_7$, and Lithium Metaphosphate $LiPO_3$. However, these phases show low enough conductivity to be applied as a solid electrolyte to the battery. Research on the development of phosphate oxide-based solid electrolytes in the Li_2O-P_2O_5 system has been widely reported in the form of scientific articles. All these studies are carried out in a variety of compound formation compositions, using various characterization techniques, to investigate various aspects of solid electrolyte composition, including microstructure, physical properties, thermal properties, and electrochemical properties, to find ideal solid electrolytes stable with good performance to be applied in a cell (Jodi *et al.,* 2017).

The approaches to increase the conductivity are mostly done by adding one or more other metal oxides, such as aluminium, titanium, etc., into new alloys, or modifying them into composites, with the addition of carbonates or sulphates (Raguenet *et al.*, 2012; Xie *et al.,* 2022; Purwamargapratala *et al.,* 2019). All approaches have one thing in common: creating defects or disorders within the material framework. That is because irregularities or defects up to a certain concentration in the material provide more space for ions to move and polarize so it is expected to be able to increase its conductivity. The addition of clay montmorillonite to Li_3PO_4 compounds to form composites increased the conductivity of the compound (Jodi *et al.,* 2016; Purwamargapratala *et al.*, 2022; Takahashi *et al.*, 2013). The conductivity of the Li_2O-P_2O_5 compound also was improved by modifying the composition from stoichiometry (Muhammad *et al.*, 2020). The deviation from the stable phase composition makes some materials do not react with other precursors but it reacts with the gas in the environment. This can cause oxidation or reduction reactions, which result in defects or impurity phases and increase the conductivity.

In this study, montmorillonite (MMT) was used as an additive to the $1.5Li_2O$-P_2O_5 compound which is a composition that deviates from the stable phase of $Li_4P_2O_7$. MMT is a soft phyllosilicate microcrystalline mineral that can be found in almost all corners of the world and can be extracted from bentonite. MMT has a multi-layered structure in which two tetrahedral silicate layers and an octahedral Aluminate layer form flat plate sheets in a sandwich configuration, in which between the plate sheets are cavities that can be filled with cations, as well as water molecules. This structure is expected to be able to store or receive ions from the outside, or in other words, be a pathway for ion movement. Free space and weak bonds between atoms in the MMT structure are expected to make it easier for atoms to vibrate, that matter can be proven by looking at the value of the dielectric characteristic of the new composite. How far the addition of MMT to the Li_2O-P_2O_5 system will influence the dielectric performance of the system and its conductivity, further research is needed. This study was conducted determine the effect of adding MMT affects the process of forming $1.5Li_2O$-P_2O_5-MMT compound, and whether it influences the electrical properties and permittivity of the compound.

2. Experimental method

2.1. Materials

Li_2CO_3 (Lithium Carbonate, Alfa Caesar, 99%), and $NH_4H_2PO_4$ (Ammonium dihydrogen Phosphate, Merck, 98%) were the precursors used to synthesize the Li_2O-P_2O_5 compound. The clay used in this study was Montmorillonite K10 (MMT K10, Sigma Aldrich). Supporting materials that were widely used are silver paste as a current collector in EIS measurements, liquid Nitrogen as a quenching medium, Stainless Steel dyes for pellet powder samples, and the furnace for the heating and sintering process. Digital scales, magnetic stirrers, ceramic mortar, glass and ceramic cups, bakers and plates, spatulas, etc., were the laboratory tools used during preparation and synthesis.

2.2. Sample preparation

The precursors were weighted with a digital scale based on a predetermined composition of $1.5Li_2O$-P_2O_5, while the MMT clay was added in certain compositions by wt%. All were mixed using a magnetic stirrer for 2 hours and then heated gradually to a temperature of 650 °C, to remove components that are not needed in the reaction. For the solid-state reaction of $1.5Li_2O$-P_2O_5, there is a phase change of around 630 °C from β-$Li_4P_2O_7$ + $LiPO_3$ phases to α-$Li_4P_2O_7$ + liquid phases (Masaki Shimoda, *et al.,* 2022). The mixture was held for two hours at the reaction temperature and then rapidly quenched in liquid nitrogen. After being ground using a mortar for 1 hour, the mixture was dried at 80 °C for 4 hours. A part of the powder samples was formed into cylindrical pellets with a diameter of 15 mm, using press machines with a pressure of 6000 psi. Each sample is coded as LMKxx which means Lithium Phosphate MMT ($1.5Li_2O$-P_2O_5-MMT) composite with a total MMT content of xx wt%.

2.3. SEM characterization

SEM equipment integrated with EDS from JEOL, JSM 6510LA was used to take the micrograph photos of the samples for morphological characterization and elemental analysis. The powder samples were affixed to a double tape and coated with gold used for this characterization. The resulting photo from the SEM is generated from electrons being fired at the surface of the sample. The result of the interaction between electrons and atoms on the surface of the sample in the form of Back Scattering electrons, Secondary electrons, or X-rays, is captured by the detector and converted into an image that can be seen on the monitor.

The EDS (Energy Dispersive X-Ray Spectroscopy) testing was then carried out to see the elemental composition present in certain spots, which will be used as a test value to determine the composition of the compounds in the samples.

2.4. Hygroscopicity characterization

Hygroscopicity characterization quantitatively was carried out by weighing method (Muhammad *et al.*, 2020). Although it depends on the accuracy and reliability of weight balance, this technique has advantages such as accessible and easy preparation, suitable for more than one form of sample, and does not require a special shape or form of sample. The pelleted sample was weighed and placed on a glass slide and put in an enclosed chamber with a specified relative humidity of 95% and

left exposed to the air in the chamber. After a predetermined amount of time, the sample is then weighed again to measure the change in sample weight before and after being exposed to the air. The level of hygroscopicity is then calculated by considering the change in the sample weight and the surface area of the sample exposed to the air.

2.5. Impedance Spectroscopy characterization

HIOKI 3532-50 LCR meter (Electrochemical Impedance Spectrometer) was used to characterize the electrical properties of the samples. A pelleted sample was held in sandwich geometry by silver paste electrodes. The impedance of the sample was measured within the 42 Hz to 5 MHz frequency range in ambient temperature. The output data, namely impedance value Z and phase angle θ, is then plotted in the form of a Nyquist plot as the relationship between the real part of the impedance and the imaginary part of the impedance. The value of solution resistance R is obtained from the intersection of the impedance loop with the x-axis, the relaxation frequency ω is from the frequency at the peak of the circular arc, while the capacitance value is calculated from the resistance value and the relaxation frequency using the equation 1.

$$\tau = RC = \frac{1}{\omega_r} \quad (1)$$

Conductivity data were calculated from the impedance considering the sample constant, using the formula (Eq 2),

$$\sigma = \frac{1}{R_p}\frac{d}{A} \quad (2)$$

where Rp, d, and A are the sample polarization resistance, sample thickness (the distance between the electrodes), and the interface area between the sample and electrode. Plotted conductivity data as a frequency function was then fitted to the formula of Jonschers universal power Law (Eq 3) to get the value of dc conductivity

$$\sigma(\omega) = \sigma_{dc} + A\omega^s \quad (3)$$

where $\sigma(\omega)$ is total conductivity, σ_{dc} is the direct current conductivity of the sample, and $A\omega^s$ is the pure dispersive component of ac conductivity. The equation for the complex permittivity is given as (Eq 4),

$$\varepsilon^*(\omega) = \varepsilon' + i\varepsilon'' = \frac{Z''}{(Z')^2 + (Z'')^2} + i\frac{Z'}{(Z')^2 + (Z'')^2} \quad (4)$$

where ε*(ω) is complex permittivity, while Z is complex impedance. The ' and " signs indicate the real part and the imaginary part of the impedance (Z) and permittivity (ε).

3. Results and discussion

Figure 1 shows the SEM micrographs of $1.5Li_2O$-P_2O_5-MMT composites produced from a secondary electron beam. The LMK00 surface has a glassy surface covered in flakes that may have come from quenched melt $LiPO_3$ glass. The surface shape of the flake was still seen on the surface of the LMK10 sample with 10% by weight MMT content. As the MMT content is added, the shape of the flake is reduced and appears to be an elongated dense lump (like a pillar) at 20% by weight MMT content. The lump size is getting clearer and bigger on larger MMT content. This may be related to the ability of MMT to absorb liquid during the reaction process.

In the synthesis of the $1.5Li_2O$-P_2O_5 compound through the melt-quench solid reaction, a minor $LiPO_3$ phase is produced, as the solid reaction process will follow the phase diagram provided by Ayu. (Ayu *et al.,* 2016). At temperatures below 600 °C, the reaction will produce a mixed phase of $Li_4P_2O_7$ + $LiPO_3$. As the temperature rises, the $LiPO_3$ phase turns to liquid, and at above 630°C, only the monoclinic $Li_4P_2O_7$ phase remains.

In the reaction without MMT, the liquid phase which has not reacted completely returns to glassy $LiPO_3$ flakes when the mixture is quenched. However, when MMT particles are added to the reaction, the liquid phase may be mixed (or absorbed) into the MMT cavity, forming a solid granular-like pillar. Because this liquid phase is evenly dispersed, as the temperature increases, evaporation of this phase is faster and more evenly distributed, producing large solid large pillars.

Elemental analysis of LMK00 using EDS provides an EDS diagram pattern which is dominated by Phosphorus and Oxygen, that interprets the Li_2O-P_2O_5 phases. The composition of Phosphorus and Oxygen are respectively 23.38 and 76.62 at%, implying that the alloy is dominated by the $Li_4P_2O_7$ phase, which is in accordance with the result analysis conducted by Jodi (Jodi *et al.*, 2021). For LMK composites with MMT content, the EDS diagram shows the Aluminium and Silicon peaks in addition to the Phosphorus and Oxygen, which imply the presence of an aluminium-silicate layer of MMT. The composition of elements on LMK compounds from the EDS scan is summarized in Table 1 which shows that the Aluminium and Silicon compositions increased with increasing MMT content.

Some phases of the Li_2O-P_2O_5 compound exhibit high hygroscopic properties such as the $LiPO_3$ phase. Figure 2a shows the change in mass of the LMK samples when placed in an environment with high humidity of 95%, for 24 hours and 144 hours. The first 24 hours showed that the LMK10 sample indicates a higher level of mass change due to water vapor absorption compared to other samples. This is probably because in the LMK10 sample there are still many $LiPO_3$ glassy phases as shown by SEM results, so the vapor absorption occurs by two phases together, namely $LiPO_3$ and MMT. However, after 144 hours, along with the addition of MMT content, there was a tendency to decrease the change in sample mass. It stated that the addition of MMT content can reduce the rate of absorption of water vapor, which means reducing the hygroscopicity level as explained by the average rate of absorption of water vapor as shown in Figure 2b.

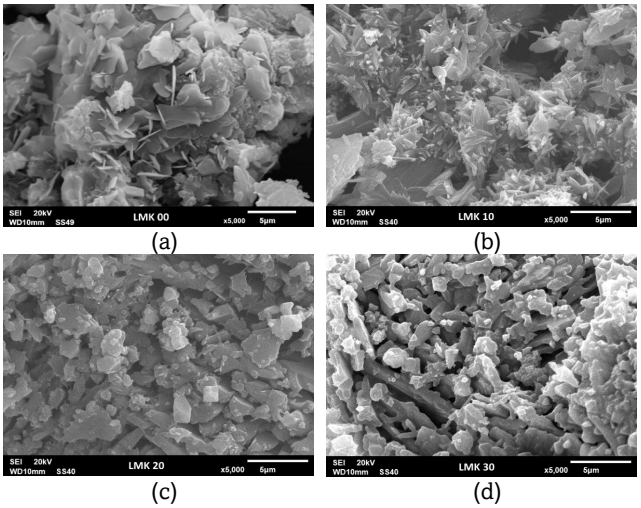

Fig 1. SEM micrographs of LMK samples. (a) $1.5Li_2O$-P_2O_5 with no MMT addition, (b) 10 wt%, (c) 20 wt%, and (d) 30 wt% MMT addition.

Table 1
The composition of elements on LMK samples.

Atomic %	LMK00	LMK10	LMK20	LMK30
Oxygen-O	76.62	73.37	71.28	66.03
Phosphorus-P	23.38	21.85	19.15	20.03
Aluminium–Al	---	0.62	0.72	1.77
Silicon-Si	---	4.16	8.85	12.17

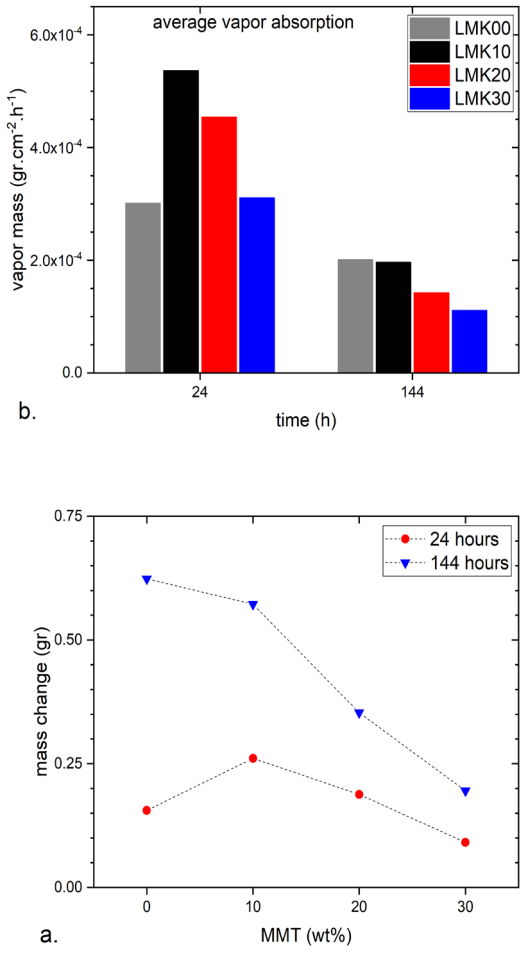

Fig 2. Water vapor absorption characteristic of LMK samples. a). the change in mass of samples in high humidity environment, and b). the average rate of water vapor absorption.

Figure 3. shows the Nyquist impedance plot of LMK composite samples measured at room temperature, which depicts the response of the material to the electric field applied to the sample. The whole curve in Figure 3 can be said to consist of only an imperfect semi-circular arc, which indicates that in all samples only one relaxation process occurs. The intersection of the impedance loop with the x-axis indicates the resistive properties of the material or solution resistance, which shows that the LMK30 has the highest value, while the LMK20 has the smallest resistance value. Similarly, the sample with 30 w% MMT content has the highest value of the capacitive impedance. The real part (resistive) and the imaginary part (capacitive) impedance values for each sample are summarized in Table 2, which are calculated from the experimental data plot that is fitted to the circle arc equation using data analysis and Graph Plotting Software. The capacitance value is calculated using equation (1) considering the relaxation frequency and the resistance. The capacitance of all arcs is in the order of pF (picofarad), which indicates that the main contribution of the response that occurs in the sample is the response of the bulk material (Taher *et al.*, 2016).

Figure 4 shows the impedance behaviour as a function of frequency. The resistive impedance of the LMK sample decreases with increasing frequency and is followed by a steep decrease to a certain impedance value. At higher frequencies, the resistive impedance values are likely to be coincident at low values as an indication of the charge release process (Jodi *et al.*, 2017).

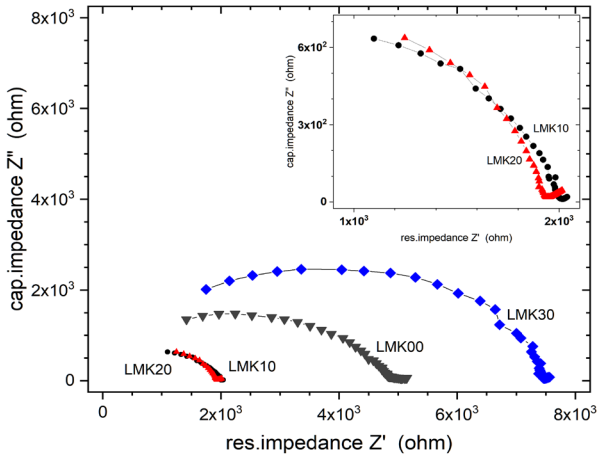

Fig 3. Nyquist impedance plot of LMK composite samples

Table 2
Impedance parameters calculated from Nyquist impedance plot.

Impedance parameter		LMK00	LMK10	LMK20	LMK30
Resistance	R_b (Ω)	$4.91x10^{+3}$	$2.01x10^{+3}$	$1.94x10^{+3}$	$7.51x10^{+3}$
Relaxation frequency	ω (Hz)	$1.21x10^{+7}$	$2.47x10^{+7}$	$3.14x10^{+7}$	$1.21x10^{+7}$
Relaxation time	τ (s)	$8.26x10^{-8}$	$4.04x10^{-8}$	$3.18x10^{-8}$	$8.26x10^{-8}$
Capacitance	C_b (F)	$1.68x10^{-11}$	$2.01x10^{-11}$	$1.64x10^{-11}$	$1.10x10^{-11}$

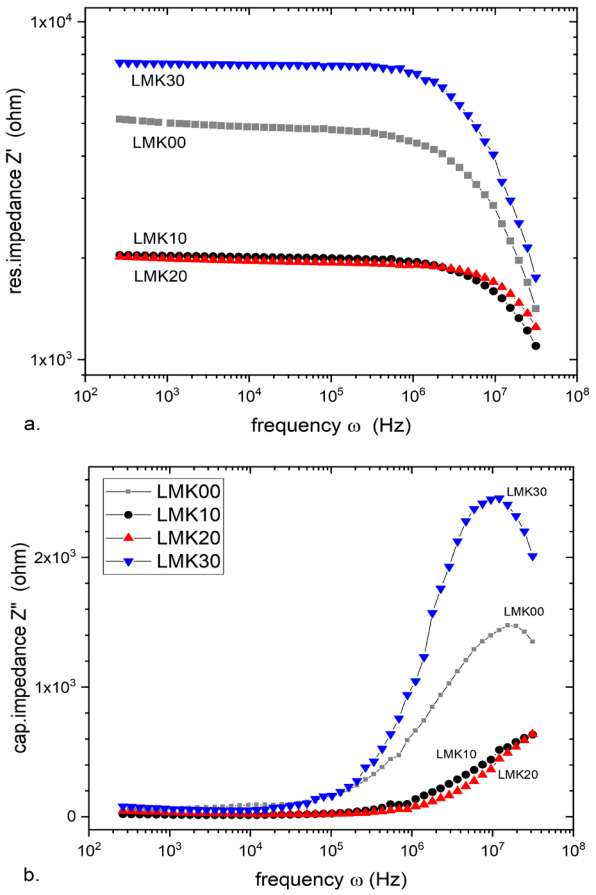

Fig 4. The impedance behaviour of LMK composite samples as a function of measurement frequency. a). real part of impedance plot., b) imaginary part of impedance.

The capacitive impedance behaviour of LMK samples is characterized by the appearance of peaks at higher frequencies. This shows the existence of a relaxation process in the sample (Subohi *et al.*, 2016). The LMK30 has a larger capacitive impedance compared to other LMK samples, while the lowest capacitive impedance is owned by the LMK20. The peak impedance frequency (relaxation frequency) value shifted towards a greater frequency as the capacitive impedance value decreased, indicating the relaxation time is getting shorter. It indicates that the LMK20 compound has a faster time to reach a new equilibrium in response to an applied electric field compared to other compositions (Thomas *et al.*, 2017). The addition of MMT content to the compound is estimated to add immovable ion content in the dielectric sample of the Li_2O-P_2O_5 compound and facilitate the relaxation process. Because in the dielectric material, in general, the relaxation process occurs due to the presence of an immovable charge at low temperatures and due to the presence of defects or vacancies at high temperatures (Sen *et al.*, 2008).

The conductivity curves of LMK composite alloys as a function of measurement frequency are shown in Figure 5. The conductivity of each frequency point on this curve is calculated from the measured impedance value. The complex conductivity curves of all samples have two parts of an area, namely the area where the conductivity forms a near-plateau region and the area where the conductivity value increases with increasing frequency. The near-plateau region marks dc conductivity where conductivity is independent of the frequency, while the second one is ac conductivity which is frequency dependent (Jayswal *et al.*, 2013). The ac conductivity indicates the material's hopping ion conduction mechanism (Sassi *et al.*, 2015), and has characteristics of power law in terms of angular frequency ($A\omega^s$) where s is the degree of interaction between mobile ions and the lattices around them ($0 \leq s \leq 1$), and A is a constant which determines the strength of polarizability (Dhahri *et al.*, 2018). The conductivity values are obtained by fitting the measurement curves in Figure 6 to equation (3). The fitted conductivity values are described as the dotted line curve in Figure 5 and summarized in Table 3.

The conductivity of the compound increases with the addition of MMT and reaches a maximum in the LMK20. Further addition of MMT content decreases the conductivity value to smaller order than before the addition. The LMK conductivity with MMT content up to 20wt% is in order of 10^{-4} S/cm, two orders higher than that of the $2Li_2O$-P_2O_5 compound, and 4-5 orders higher than the conductivity of the Li_3PO_4 compound (Jodi *et al.*, 2016). The exponential power value of all alloys is in the range of value s = 0.63 ~ 0.78. This value approaches the exponent value for the conductivity of glass material which contains a high alkaline content of s≈0.6, which is measured in the kHz ~ MHz frequency range at room temperature (Jodi *et al.*, 2017).

That is clearly seen that the addition of MMT is not linearly correlated with changes in the impedance and conductivity of the material. The morphology of the sample shows that the MMT acts as a medium that absorbs the liquid in the reaction, thereby accelerating the formation of the desired phase. Jodi et al stated that the addition of MMT to a certain level reduces the formation of the $LiPO_3$ and increases the formation of the $Li_4P_2O_7$ which has high conductivity and is the dominant phase determining the total conductivity (Heri Jodi. *et al.*, 2021) However, more detailed research is needed to determine the direct correlation of changes in MMT volume to changes in $Li_4P_2O_7$ conductivity. Further addition of MMT makes its own conductivity affect the total conductivity to be lower than the conductivity of the dominant phase.

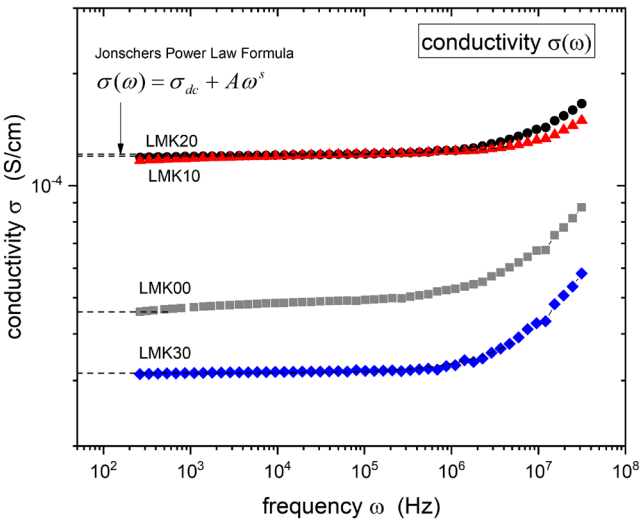

Fig 5. The complex conductivity plot of LMK samples.

Table 3
The permittivity value of LMK samples at f=42 Hz.

Permittivity Parameters		LMK00	LMK10	LMK20	LMK30
Dielectric constant	ε' (F/m)	$1.03x10^{+5}$	$4.98x10^{+4}$	$1.13x10^{+5}$	$1.42X10^{+4}$
Dielectric loss slope	*m*	-0.96	-0.98	-0.99	-0.97
tandelta	*D*	52.50	165.78	103.06	149.04

4. Conclusion

The addition of MMT content to the $1.5Li_2O$-P_2O_5 compound formed a new $1.5Li_2O$-P_2O_5-MMT (LMK) electrolyte composite. MMT content in LMK composites influences the morphology of the compound which changes from a structure covered in glassy shapes to pillar-like lumps. It is believed that MMT acts as a medium that absorbs the liquid phase in the solid-state reaction and forms pillar-like lumps. EDS analysis shows the predominance of Oxygen and Phosphorus elements in all LMK compounds, where there is an increase in the content of Aluminium and Silicon elements along with the addition of MMT content. The impedance response of all compounds is dominated by the grain response, indicated by a semi-circle on the impedance curve, and picofarad order of capacitance value. The bulk resistance shows a decrease along with the addition of MMT content, and reaches a minimum in the LMK20 composition, indicating the highest conductivity in the order of 10^{-4} S/cm. LMK20 composites become the most polarizable and dielectric compound, which is shown by the smallest relaxation time of $3.18x10^{-8}$ (s), and the highest dielectric constant of $1.13x10^{5}$.

Acknowledgment

There is no conflict of interest in the writing of this paper. We greatly appreciate the financial support from the Ministry of Research, Technology, and Higher Education of the Republic of Indonesia and our gratitude goes to the Research Center for Advanced Materials, the National Research, and Innovation Agency, and the Department of Metallurgical and Materials Engineering, the University of Indonesia for their support.

References

Ayu, N. I. P., Kartini, E., Prayogi, L. D., Faisal, M., Supardi. (2016). Crystal structure analysis of Li_3PO_4 powder prepared by wet chemical reaction and solid-state reaction by using X-ray diffraction (XRD). *Ionics,* 22(7), 1051-1057. https://doi.org/10.1007/s11581-016-1643-z

Das, S. S., Singh, N. P., Srivastava, V., and Srivastava, P. K. (2008). Synthesis, electrical conduction and structure–property correla-tion in $(50-x)Ag_2O–50P_2O_5–xCoCl_2$ glassy systems. *Solid State Ion*, 179(40), 2325–2329. https://doi.org/10.1016/j.ssi.2008.09.018 .

Deka, M. and Kumar, A. (2011). Electrical and electrochemical studies of poly (vinylidene fluoride)–clay nanocomposite gel polymer electrolytes for Li-ion batteries. *Journal Power Sources*, 196(3), 1358–1364. https://doi.org/10.1016/j.jpowsour.2010.09.035 .

Dhahri, A., Dhahri, E., & Hlil, E. K. (2018). Electrical conductivity and dielectric behaviour of nanocrystalline $La_{0.6}Gd_{0.1}Sr_{0.3}Mn_{0.75}Si_{0.25}O_3$. *Royal Society of Chemistry Advances,* 8(17), 9103–9111. https://doi.org/10.1039/c8ra-00037a

Fang, S., Bresser, D., & Passerini, S. (2019). Transition Metal Oxide Anodes for Electrochemical Energy Storage in Lithium- and Sodium-Ion Batteries. *Advanced Energy Materials,* 1902485. https://doi.org/10.1002/aenm.201902485

Guo, Y., Wu, S., He, Y., Kang, F., Chen, L., Li, H., Yang, Q. (2022). Solid-state lithium batteries: Safety and prospects, *eScience,* 2(2),138-163, https://doi.org/10.1016/j.esci.2022.02.008.

Hartmann, P., Rosenberg, M., Juhasz, Z., Matthews, L. S., Sanford, D. L., Vermillion, K., Carmona-Reyes, J., and Hyde, T. W. Ionization Waves In The Pk-4 Direct Current Neon Discharge. (2020). *Plasma Sources Science and Technology*. 29. 115014. https://doi.org/10.1088/1361-6595/abb955

Hou, Q., Buckeridge, J., Lazauskas, T., Mora-Fonz, D., Sokol, A. A., Woodley, S. M., & Catlow, R. C. A. (2018). Defect formation in In_2O_3 and SnO_2: a new atomistic approach based on accurate lattice energies. *Journal of Materials Chemistry C*. 6, 12386-12395. https://doi.org/10.1039/c8tc04760j

Jayswal, M. S., Kanchan, D. K., Sharma, P., and Gondaliya, N. (2013). Relaxation process in $PbI_2–Ag_2O–V_2O_5–B_2O_3$ system: Dielectric, AC conductivity and modulus studies. *Materials Science and Engineering: B*, 178(11), 775–784. https://doi.org/10.1016/j.mseb.2013.03.013

Jodi H., Supardi, Kartini, E., and Zulfia, A. (2016). Synthesis and Electrochemical Characterization of Li_3PO_4 for Solid State Electrolytes. *Jurnal Sains Materi Indonesia*, 18(1), 1–8. https://doi.org/10.17146/jsmi.2016.18.1.4181

Jodi H., Zulfia, A., Deswita, and Kartini, E. (2016). A Study of the Structural and Electrochemical Properties of Li_3PO_4-MMT-PVDF Composites for Solid Electrolytes. *International Journal of* Technology, 7(8), 1291–1300. https://doi.org/10.14716/ijtech. v7i8.6894.

Jodi, H., Syahrial, A. Z., Sudaryanto, and Kartini, E. (2017). Synthesis and electrochemical charac-terization of new Li_2O-P_2O_5 compounds for solid electrolytes. *International Journal of Technology*, 8(8). https://doi.org/10.14716/ijtech. v8i8.681.

Jodi, H., Syahrial, A.Z., Sudaryanto, S., Kartini, E.., (2017). Synthesis and Electrochemical Characterization of New Li_2O-P_2O_5 Compounds for Solid Electrolytes. *Interna-tional Journal of Technology*. 8(8),1516-1524.https://doi.org/10.14716/ijtech.v8i8.681

Jodi, H., Yulianti, E., Sudjatno, A., Syahrial, A. Z., and Kartini, E. (2021). Blending Effect in Li_2O-P_2O_5-MMT Solid Electrolyte and Its Contribution to Conductivity Value. *AIP Conference Proceedings* 2381, 020025. https://doi.org/10.1063/ 5.0066611

Kartini, E., Honggowiranto, W., Supardi, Jodi, H., and Jahya, A. K., Wahyudianingsih (2014). Synthesis and Characterization of New Solid Electrolyte Layer $(Li_2O)_x(P_2O_5)_y$. *14th Asian Conference on Solid State Ionics,* 2, 163–173. https://doi.org/10.3850/978-981-09-1137-9_147.

Kartini, E., Nakamura, M., Arai, M., Inamura, Y., Nakajima, K., Maksum, T., Honggowiranto, W., Putra, T.Y.S.P., (2014). Structure and dynamics of solid electrolyte $(LiI)_{0.3}(LiPO_3)_{0.7}$. *Solid State Ion*, 262,833–836. https://doi.org/10.1016/j.ssi.2013.12.041 .

Kaur, G., Singh, M. D., Sivasubramanian, S. C., & Dalvi, A. (2022). Investigations on enhanced ionic conduction in ionic liquid dispersed sol-gel derived $LiTi_2(PO_4)_3$. *Materials Research Bulletin, 145,111555.*https://doi.org/10.1016/j. materresbull.2021.111555

Knauth, P., (2009). Inorganic solid Li ion conductors : An overview. *Solid StateIon*, 180(14–16), 911–916. https://doi.org/10.1016/j.ssi. 2009.03.022 .

Koniak, M., & Czerepicki, A. (2017). Selection of the battery pack parameters for an electric vehicle based on performance requirements. *IOP Conference Series: Materials Science and Engineering,* 211, 012005. https://doi.org/10.1088/1757-899x/ 211/1/012005

Kuznetsov, O. A., Mohanty, S., Pigos, E., Chen, G., Cai, W., Harutyunyan, A. R. (2022). High energy density flexible and

ecofriendly lithium-ion smart battery. *Energy Storage Materials,* 54, 266-275, https://doi.org/10.1016/j.ensm.2022.10.023.

Lin, X., Zhou, G., Liu, J., Yu, J., Effat, M. B., Wu, J., & Ciucci, F. (2020). Rechargeable Battery Electrolytes Capable of Operating over Wide Temperature Windows and Delivering High Safety. *Advanced Energy Materials,* 2001235. https://doi.org/10.1002/aenm.202001235

Ohno, S., Rosenbach, C., Dewald, G. F., Janek, J., & Zeier, W. G. (2021). Linking Solid Electrolyte Degradation to Charge Carrier Transport in the Thiophosphate-Based Composite Cathode toward Solid-State Lithium-Sulfur Batteries. *Advanced Functional Materials,*31(18),2010620. https://doi.org/10.1002/adfm.202010620

Pang, Y., Pan, J., Yang, J., Zheng, S., & Wang, C. (2021). Electrolyte/Electrode Interfaces in All-Solid-State Lithium Batteries: *A Review. Electrochemical Energy Reviews,* 4(2), 169–193. https://doi.org/10.1007/s41918-020-00092-1

Purwamargapratala, Y., Gunawan, I., Kartini, E., Zulfia, A., Glushshenkov, A., Haerani, D., & Sudirman, S. (2022). Effect of Sodium in $LiNi_{0,5}Mn_{0,3}Co_{0,2}O_2$ as a Lithium Ion Battery Cathode Material by Solid State Reaction Method. *Journal of Fibers and Polymer Composites*, 1(1), 66–72. https://doi.org/10.55043/ jfpc.v1i1.41

Purwamargapratala, Y., Sudaryanto, & Akbar, F. (2020). Neutron tomography study of a lithium-ion coin battery. *Journal of Physics: Conference Series,* 1436, 012029. https://doi.org/10.1088/1742-6596/1436/1/012029

Purwamargapratala, Y., Sujatno, A., Sabayu, Y. L., & Kartini, E. (2019). Synthesis of $Li_4Ti_5O_{12}$ (LTO) by Sol-Gel Method for Lithium-Ion Battery Anode. *IOP Conference Series: Materials Science and Engineering,* 553, 012062. https://doi.org/10.1088/1757899x/ 553/1/012062.

Quartarone E. and Mustarelli, P. (2011). Electrolytes for solid-state lithium rechargeable batteries: recent advances and perspectives. *Chemical Society Reviews,* 40(5), 2525–2540. https://doi.org/10.1039/C0CS00081G .

Radoń, A., Łukowiec, D., Kremzer, M., Mikuła, J., & Włodarczyk, P. (2018). Electrical Conduction Mechanism and Dielectric Properties of Spherical Shaped Fe_3O_4 Nanoparticles Synthesized by Co-Precipitation Method. *Materials,* 11(5), 735. https://doi.org/ 10.3390/ma11050735

Raguenet B., Tricot, G., Silly, G., Ribes, M., and Pradel, A. (2012). The mixed glass former effect in twin-roller quenched lithium borophosphate glasses. *Solid State Ion,* 208, 25–30. https://doi.org/ 10.1016/j.ssi.2011.11.034 .

Riza, M. A., Go, Y. I., Maier, R. J. R., Harun, S. W., and Anas, S. B. (2020). Hygroscopic Materials and Characterization Techniques for Fiber Sensing Applications: A Review. *Sensors and Materials*, 32(11), 3755–3772. https://doi.org/10.18494/SAM.2020.2967

Sahu, G., Lin, Z., Li, J., Liu, Z., Dudney, N., and Liang, C. (2014). Air-stable, high-conduction solid electrolytes of arsenic-substituted Li_4SnS_4. *Energy Environ Science,* 7(3), 1053–1058, https://doi.org/10.1039/C3EE43357A

Sassi, M., Bettaibi, A., Oueslati, A., Khirouni, K., and Gargouri, M. (2015). Electrical conduction mecha nism and transport properties of $LiCrP_2O_7$ compound. *Journal Alloys Compounds*, 649, 642–648. https://doi.org/10.1016/j.jallcom.2015.07.148 .

Sen, S., Mishra, S. K., Palit, S. S., Das, S. K., & Tarafdar, A. (2008). Impedance analysis of $0.65Pb(Mg_{1/3}Nb_{2/3})O_3$–$0.35PbTiO_3$ ceramic. *Journal of Alloys and Compounds,* 453(1-2), 395–400. https://doi.org10.1016/j.jallcom.2006.11.126

Shimizu, K., Nyström, J., Geladi, P., Lindholm-Sethson, B., & Boily, J.-F. (2015). Electrolyte ion adsorption and charge blocking effect at the hematite/aqueous solution interface: an electrochemical impedance study using multivariate data analysis. *Physical Chemistry Chemical Physics,*17(17), 11560–11568. https://doi.org/10.1039/c4cp05927a .

Shimoda, M., Maegawa, M., Yoshida, S., Akamatsu, H., Hayashi, K., Gorai, P., and Ohno, S. (2022). Controlling Defects to Achieve Reproducibly High Ionic Conductivity in Na_3SbS_4 Solid Electrolytes. *Chemichal. Materials*. (2022). 34, 12, 5634–5643. https://doi.org/10.1021/ acs.chemmater.2c00944

Subohi, O., Bowen, C. R., Malik, M. M., and Kurchania, R. (2016). Dielectric spectroscopy and ferroelectric properties of magnesium modified bismuth titanate ceramics. *Journal of Alloys and Compounds*, 688(B), 27–36. https://doi.org/10.1016/j.jallcom.2016.07.173

Sudaryanto, Yulianti, E., and Jodi, H. (2015). Studies of Dielectric Properties and Conductivity of Chitosan-Lithium Triflate Electrolyte. *Polymer Plastic Technology Engineering,* 54(3),290–295. https://doi.org/10.1080/03602559.2014.977424 .

Taher, Y.B., Moutia, N., Oueslati, A., and Gargouri. M. (2016). Electrical properties, conduction mechanism and modulus of diphospha te compounds. *Royal Society of Chemistry Advances*, 6(46), 39750–39757. https://doi.org/10.1039/C6RA05220G.

Takahashi, C., Shirai, T., Hayashi, Y., & Fuji, M. (2013). Study of intercalation compounds using ionic liquids into montmorillonite and their thermal stability. *Solid State Ionics, 241, 53–61*. https://doi.org/10.1016/j.ssi.2013.03.032

Thomas, A. K., Abraham, K., Thomas, J., & Saban, K. V. (2017). Electrical and dielectric behaviour of $Na_{0.5}La_{0.25}Sm_{0.25}Cu_3Ti_4O_{12}$ ceramics investigated by impedance and modulus spectroscopy. *Journal of Asian Ceramic Societies,* 5(1), 56–61. https://oi.org/10.1016/j.jascer.2017.01.002

Triyono, D., Fitria, S. N., & Hanifah, U. (2020). Dielectric analysis and electrical conduction mechanism of $La_{1-x}Bi_xFeO_3$ cera-mics. *Royal Society of Chemistry Advances,* 10(31), 18323–18338. https://doi.org/10.1039/ d0ra02402

Usiskin, R., & Maier, J. (2020). Interfacial Effects in Lithium and Sodium Batteries. *Advanced Energy Materials,* 2001455. https://doi.org/10.1002/aenm.202001455

Wu, F., Chen, N., Chen, R., Zhu, Q., Qian, J., & Li, L. (2016). "Liquid-in-Solid" and "Solid-in-Liquid" Electrolytes with High-Rate Capacity and Long Cycling Life for Lithium-Ion Batteries. *Chemistry of Materials,* 28(3), 848–856. https://doi.org/10.1021/acs. Chem mater.5b04278

Xiayin. Y., Bingxin H., Jingyun Y., Gang P., Zhen H., Chao G., Deng L., and Xiaoxiong. (2016). All-solid-state lithium batteries with inorganic solid electrolytes: Review of fundamental science. *Chinese Physics B*, 25(1), 18802. https://doi.org/10.1088 /1674-1056/25/1/018802

Xie, W., Wei, S., Hudon, P., Jung, I.-H., Qiao, Z., & Cao, Z. (2020). Critical evaluation and thermodynamic assessment of the R_2O–P_2O_5 (R = Li, Na and K) systems. *Computer Coupling of Phase Diagram and Thermochemistry,* 68, 101718 https://doi.org/10.1016/j.calphad.2019.101718

Zhao, Y., Wang, L., Zhou, Y., Liang, Z., Tavajohi, N., Li, B., & Li, T. (2021). Solid Polymer Electrolytes with High Conductivity and Transference Number of Li Ions for Li-Based Rechargeable Batteries. *Advanced Science,* 8(7), 2003675. https://doi.org/10.1002/advs.202003675